Journal of Polymers and the Environment (2022) 30:3701–3717
https://doi.org/10.1007/s10924-022-02465-7

ORIGINAL PAPER

Recycling Expanded Polystyrene with a Biodegradable Solvent to Manufacture 3D Printed Prototypes and Finishing Materials for Construction

Suellen Signer Bartolomei[1] · Felipe Lopes Fonseca da Silva[2] · Esperidiana Augusta Barreto de Moura[3] · Hélio Wiebeck[4]

Accepted: 25 April 2022 / Published online: 14 May 2022

Abstract

The amount of plastic waste generated is causing damage to the environment, such as sea and soil pollution, and one of the alternatives for disposing of polymers is recycling. This work proposes recycling expanded polystyrene using a biodegradable solvent, its plastification with glycerol, and the preparation of the composite with post-consumer recycled gypsum for applications to manufacturing by 3D printing and for finishing materials for construction. Specimen for tensile testing and shore D hardness were prepared by injection process and by 3D printing. In addition, Thermogravimetric (TG), Fourier-transform infrared spectrometry (FTIR), Differential scanning calorimeter, Scanning electron microscope (FESEM) analyses, and flame propagation tests were also carried out. TG and FTIR analyses show that the recycling process did not degrade the material, and the addition of glycerol and gypsum improved the thermal stability of the composite. The mechanical properties of the injected and 3D printed samples with gypsum were similar, due to the dimensional stability of the manufactured filament, which improved the speed and quality of the specimen printing. The increase in ductility and the reduction in the glass transition temperature showed that the recycled expanded polystyrene (RPS) were effectively plasticized with the addition of 2 wt% glycerol, preserving their flame self-extinguishment when subjected to the flame propagation test. Due to these properties, the plasticized RPS can be used to manufacture articles for finishing in civil construction, and the RPS composite can be used to manufacture 3D printed prototypes.

✉ Suellen Signer Bartolomei
suellen.signer@gmail.com

[1] Faculdade de Tecnologia de Sorocaba, FATEC-SO, Av. Engenheiro Carlos Reinaldo Mendes 2015, Sorocaba, SP 18013-280, Brazil

[2] Programa de Pós-Graduação em Ciência dos Materias (PPCCM), Universidade Federal de São Carlos (UFSCar), Rodovia João Leme dos Santos (SP-264), Sorocaba, SP 18052-780, Brazil

[3] Centro de Química e Meio Ambiente, Instituto de Pesquisas Energéticas e Nucleares, (CEQMA/IPEN-CNEN/SP), Av. Prof. L. Prestes 2242, São Paulo, SP 05508-000, Brazil

[4] Departamento de Engenharia Metalúrgica e de Materiais, Escola Politécnica da Universidade de São Paulo (PMT-USP), Av. Prof. Mello Moraes 2463, São Paulo, SP 05508-030, Brazil

Graphical abstract

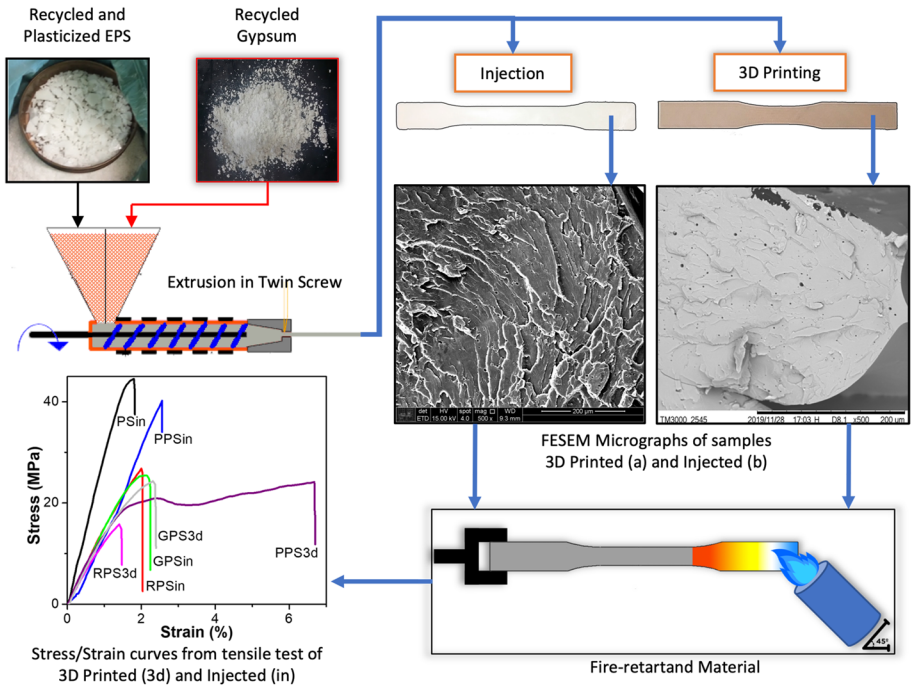

Keywords 3D printing · Recycling · Expanded polystyrene · Composite · Gypsum

Introduction

Plastics have played important roles in different industries, such as sanitation, construction, packaging, and electronics, because they are lightweight, stable, versatile and have low cost compared to other materials. In 2019, the total production of thermoplastic resins in the world was approximately 370 million tons, of which 8.2 million tons were produced in Brazil. Meanwhile, much of this material is not biodegradable for coming from petroleum, as polystyrene (PS). Among the various polymers present in the discarded waste, PS is commonly found, which can come from disposable materials, construction industry blocks and celling, packaging, among others. In Brazil, the production of products made with PS and expanded polystyrene (EPS) represented 5.7% of all resins consumed nationally in 2020 [1, 2]. In addition, incorrect disposal, and low recycling rates, around 11% worldwide, have been causing negative impacts on the environment, such as sea and soil contamination. Therefore, the study into replacing virgin polymers with recycled polymers is of great importance [1, 3].

However, the costs for the correct disposal of polymeric wastes, as well as their recycling, are high and can make the use of recycled material economically unfeasible. To enable economic gains, it is necessary that the recycled material be applied in order to value the material during its commercialization. A possible application of recycled polymers is the manufacture of filaments for three-dimensional (3D) printers [3, 4].

3D printing can economically manufacture prototypes or complex and customized components in low quantities. This production process is still too slow for large production, but obtaining of small quantities can be accelerated, 3D printing allows eliminating some steps of conventional processes, such as mold and die development, assembly and machine setup. 3D printers deposits fused thermoplastic filaments in layers at positions predefined by a computer program, according to the desired shape, allowing flexibility in design [5, 6].

However, during 3D printing manufacturing, some problems may occur due to improper setting of printing parameters, such as filament temperature and deposition speed, and defects may appear in the printed part due to filament quality: moisture, diameter variation, viscosity and flow index. Therefore, when recycling a material to make filaments for 3D printing, one must know the characteristics of the material obtained to avoid many failed printing attempts. To prevent these problems, it is very important that the diameter of the fabricated filament be constant, with small standard deviation [5, 6].

Studies show that it is possible to recycle polymers and obtain filaments with properties similar to those of commercial filaments. Zander and collaborators fabricated filaments to 3D printer using polypropylene (PP) blended with polyethylene terephthalate (PET) and PS together with compatibilizers. Tensile specimens were molded by 3D printing and the assay showed tensile strength up to 35 MPa. The mixtures showed an increase in glass transition temperature and the flexibility of PET and PS was increased by the addition of PP [7]. Spoerk et al. recycled 3D printed parts to make new filaments. This cycle was repeated 15 times to study thermal degradation due to reprocessing of 3D printed parts to obtain filaments. The authors fabricated filaments with PP, 15 wt% mineral filler and compatibilizer. Despite 15 cycles of recycling, the fillers and the polymeric matrix still presented a strong interface and a stable filament diameter was produced, but the tensile strength decreased by 20% due to chain scission. However, elastic deformation, impact resistance, rheological, morphological and thermal characteristics remained unchanged even after 15 cycles [8].

In this research paper, post-consumer recycled EPS was used as a polymeric matrix for developing filaments for 3D printing and finishing materials for civil construction. Currently, EPS is used in many areas, mainly in construction systems for slabs, thermal insulation, lightweight concrete, moldings and insulation for underfloor heating [9]. However, for these applications, the material has to present resistance to flame propagation; for this, a flame retardant is added at the time of the EPS production. The hexabromocyclododecane (HBCD) used in polystyrene foams and resins is an additive-type halogenated flame retardant, that is, it is not chemically bonded to the polymer chain and is used with a concentration between 0.3 and 0.7 wt%. Thereby, EPS can be used in civil construction, meeting international standards regarding flame propagation [10–17].

EPS can be recycled and re-expanded, but the end product is more expensive than the virgin material. Thus, most of the recycled EPS is used in solid form, to manufacture general purpose polystyrene (GPPS), or high impact polystyrene (HIPS), and molded in conventional systems, such as injection and extrusion. The most used processes for recycling EPS are mechanical, chemical and thermal recycling. The chemical recycling process allows recovering EPS through polymer solubilization, which makes it possible to remove solid contaminants using one or more filters. Industrially, the system is closed and the solvent is reused. The solvent is preferably reusable and environmentally safe. It typically has a low boiling temperature and high evaporation rate. The most used solvents are not environmentally friendly, yet it is known that organic solvents, such as toluene, benzene and others with aromatic components, are good solvents for EPS [18]. Ethyl acetate can be a more environmentally friendly alternative, because during the solubilization of the polymer, there is no significant degradation by the action of this solvent; the beads collapse due to solubility with the solvent, eliminating the air present in the material and reducing its volume. Then, the solvent can be eliminated, putting the mixture to rest, thus obtaining the rigid recycled PS. Ethyl acetate is a biodegradable solvent by the action of microorganisms, obtained by the reaction of acetic acid and ethanol in the presence of sulfuric acid and can be reused. It has a clear appearance and pleasant fruity aroma. It is soluble in water, acetone, benzene, chloroform, ethanol, ethyl ether and other chlorinated and oxygenated solvents [19–22].

Nevertheless, the material obtained after recycling EPS has low toughness and low impact strength due to its high fragility, characteristic of rigid PS [23–26]. One way to improve impact resistance is polymer plasticization, which can be accomplished by adding glycerol to the recycled EPS polymeric matrix. Previous studies have shown that glycerol, in addition to acting as a plasticizer by reducing the glass transition temperature (Tg), also inhibits crack growth during plastic deformation. Due to the high thermal conductivity of glycerol, it cools the crack, reducing the internal energy available for plastic deformation to occur. This phenomenon is amplified by capillary forces acting at the crack interface with the polymer, causing the glycerol to penetrate and distribute itself in this region, increasing the flexibility of the polymer. The increase in flexibility acts as a barrier to the crack, hindering its growth and propagation. Consequently, there is an increase in the tenacity of the PS, because a greater amount of energy will be necessary for the plastic deformation and rupture of the polymer to occur [27–30]. According to Sjoerdsma and Andreson, the glycerol must present a homogeneous dispersion in the polymer matrix, so that the plasticization is uniform throughout the polymer and thus delays the crack growth efficiently [27, 28].

Aiming at applying recycled EPS to civil construction, a number of studies have been carried out for preparing and characterizing the composites involving post-consumer EPS and gypsum residues from civil construction. These studies are stimulated by the amount of waste from gypsum mining and also by the waste from the manufacture of gypsum artifacts, such as frames [31–37].

This work aimed to recycle EPS and post-consumer gypsum, use them to manufacture a composite, and characterize them to analyze their properties and the efficiency of recycling processes. In addition, it aimed to present new applications for the recycled material, the manufacture of filaments for 3D printing and use as a finishing material for civil construction. EPS recycling was performed by solubilization in biodegradable solvent followed by processing in extruder. To improve the toughness of the recycled material, 2 wt% of glycerol was added, which acted as a plasticizer.

The composites were processed in a twin-screw extruder and specimens were molded by injection and 3D printing.

Method

Materials

Waste of Expanded Polystyrene (EPS) production from Knauf was used as a polymeric matrix. Post-consumption gypsum (calcium sulfate dihydrate) from *JR Gesso* used to obtain the composites. Ethyl Acetate ($CH_3COOCH_2CH_3$) from *Química Moderna* was used as a solvent for EPS recycling. Glycerol ($C_3H_8O_3$) from *Synth* was used as plasticizer during EPS recycling.

Gypsum Recycling

Residues from the production process of gypsum pieces were used as a source of the dispersed phase. These residues were recycled as discussed in a previous paper [38]. To that end, the gypsum post-consumption was milled, oven dried for 2 h at 100 °C and sieved to control particle size to obtain a fine, homogeneous and recycled gypsum powder.

EPS Recycling and Plastification

The ground EPS was placed in contact with biodegradable ethyl acetate in the proportion of 2 ml of solvent/1 g of polymer with the aid of a mechanical mixer [39]. After dissolution, 2 wt% glycerol was added to plasticize the polymer and was stirred for 2 h to incorporate glycerol into the polymer. The solution obtained was poured into metal containers and allowed to stand until the solvent completely evaporated. Rigid samples without air bubbles were obtained after standing and then milled in a knife mill to obtain granules of recycled material. Thus, recycled EPS with and without glycerol were obtained.

Composite and Filament Fabrication

The samples were homogenized in a Maplan twin screw extruder, the set processing temperatures were 100/105/110/115/120 °C and the rotation was 30 rpm. In the extruder, recycled gypsum powder (10 wt%) was also added for preparing a composite. Upon leaving the extruder, the material was air-cooled and pelletized. Processing in the extruder was repeated and part of the sample was again pelletized to be injected, and another part of the sample was rolled with the aid of a pull roller producing a filament with a diameter of approximately 1.75 mm.

3D Printing and Injection

The pelletized samples were molded using a YJ Brazil model YJS700 injector into mechanical test specimens, with a 200 °C injection temperature, 40 °C mold temperature and 5-s cooling time. Filament 3D printing was performed on a Voolt3D model Gi3 printer, with 15 mm/s speed, 90 °C bed temperature, 200 °C nozzle temperature, 0.4 mm nozzle thickness and 0.2-mm layer thickness. The infill percentage used for specimen printing was 100% and the print angle was 45° inverted for each layer; a linear edge was printed on the specimens. Thus, 3D-printed compositions were obtained, EPS recycled (RPS3d), EPS recycled with 2 wt% glycerol as plasticizer (PPS3d) and EPS recycled with glycerol and 10 wt% gypsum (GPS3d). The same compositions were injected and named recycled expanded polystyrene (RPS) in, PPSin, GPSin, respectively. Virgin PS was injected and named PSin. Five specimens of each composition were injected, and another five were 3D printed, according to ASTM D638. Figure 1 shows the injected and printed specimens and Table 1 shows the composition of each sample.

The filament without the plasticizer (without glycerol) was extremely fragile, breaking during filament extrusion and during specimen printing. The addition of glycerol

Fig. 1 Specimens of injected samples: expanded polystyrene recycled with glycerol and 10 wt% gypsum (GPSin); expanded polystyrene recycled with 2 wt% glycerol as plasticizer (PPSin). Specimens of 3D printed samples: GPS3d; PPS3d; expanded polystyrene recycled without glycerol (RPS3d)

Table 1 The composition of each sample

Sample	Injection	3D Printing	Glycerol (wt%)	Recycled gypsum (wt%)
PSin	x			
RPSin	x			
PPSin	x		2	
GPSin	x		2	10
RPS3d		x		
PPS3d		x	2	
GPS3d		x	2	10

reduced the material fragility, but the dimensional stability of the filament external diameter was impaired due to the appearance of bubbles, as shown in the FESEM images in "Shore D Hardness" section. The gypsum particles made the filament diameter more constant, making it possible to print faster without failures and interruptions. Recycled EPS, when heated, tends to expand due to the presence of the expanding agent, responsible for the porous formation of the material before recycling. The addition of gypsum in the recycled EPS prevented this expansion during printing, even in the presence of glycerol, which in turn, when present alone in recycled EPS caused bubbles during the printing process, destabilizing the external diameter of the filament. This phenomenon occurs because the addition of gypsum reduces the amount of volatiles present in the sample, as discussed in chapter 3.1.

The flowchart of steps for obtaining the samples to be characterized are shown in the Supplementary Information in Fig. S1.

Characterizations

Thermogravimetric analysis (TG) curves were obtained using TGA Q500 from TA Instruments. The injected samples were heated from 30 to 600 °C at a heating rate of 10 °C/min, in a nitrogen atmosphere with a flow rate of 50 ml/min. Differential scanning calorimeter (DSC) analyses were performed using DSC Q20 from TA Instruments. Firstly, the thermal history of the samples was eliminated by heating from 25 to 300 °C at a scanning rate of 10 °C/min. Subsequently, the injected samples were cooled down to room temperature at a rate of 10 °C/min. Finally, DSC curves were obtained by heating the samples from 25 to 300 °C at a rate of 10 °C/min. FTIR was employed in a Nicolet-ID5-ATR Spectrometer, in the transmission mode; the working wavenumber range of the spectrometer was from 4000 to 500 cm^{-1}. Shore D hardness tests were performed on injected and printed specimens on a Zorn Stendal model DDR8033 durometer according to DIN53505 and

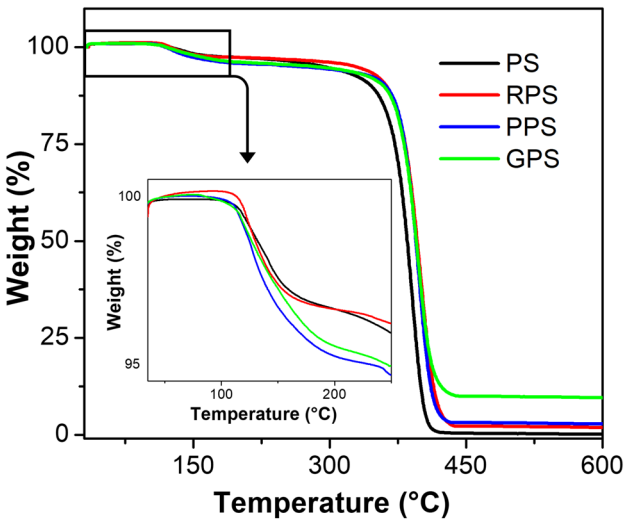

Fig. 2 TG thermograms curve; the highlighted area shows the water loss up to 200 °C, of Polystyrene (PS), Expanded polystyrene recycled (RPS), Expanded polystyrene recycled with 2 wt% glycerol as plasticizer (PPS) and Expanded polystyrene recycled with glycerol and 10 wt% gypsum (GPS)

ASTMD2240. Ten hardness readings were taken in each of the samples, using 4 overlapping specimens with a thickness of 3.2 mm each. Tensile tests of injected and 3D printed specimens were performed on a universal testing machine Instron, model 5564 according to ASTM D 638 at room temperature and loading rates of 50 mm/min. The injected and printed specimens were fractured at cryogenic temperature; the fracture region was covered with gold and observed in a scanning electron microscope (Phillips XL-30 FESEM). The flame propagation tests of the composites were performed on the injected tensile specimens in accordance with the ASTM D635 standard. Initially, the specimens were subjected to the contact of a flame for 30 s. After this time, the flame was automatically extinguished; then, the flame propagation time was timed until the flame reached the 100 mm burned sample length mark, or until it was self-extinguished by the material. Equipment of the SKZ Industrial brand, model SKZ180A horizontal textiles burning behavior tester was used for this purpose.

Results and Discussion

Thermogravimetric (TG) Analyses Results

TG analyses were performed to evaluate the thermal stability of the composites obtained and the residual weight after heating to 600 °C. Figure 2 show thermogram curves and the data collected are in Table 2.

Table 2 The loss of weight (LW) at 200 °C, the residual weight (RW) and the onset temperatures of thermal degradation (T_{onset})

Sample	LW at 200 °C (%)	RW at 600 °C (%)	T_{onset} (°C)
PS	2.7	0	363
RPS	2.7	1.8	361
PPS	4.2	2.8	374
GPS	3.9	9.0	371

The occurrence of weight loss up to 200 °C, seen in Fig. 2, can be associated with the loss of moisture present in the samples analysed. The amount of water eliminated was lower for samples that did not contain particles or glycerol. This occurred because PS is a hydrophobic material, behavior also observed in the FTIR analyses, which is in agreement with other studies. Furthermore, the weight loss shown by all prepared samples occurred in only 1 stage, demonstrating that there was no phase separation between glycerol and PSin the PPS sample. This was confirmed by the decomposition peaks in the DTG curves, seen in Fig. S2, that corresponded to the decomposition temperature, as shown in Table 2 [40].

The residual weight (RW) of the polystyrene (PS) sample was 0 wt%, while in the RPS sample it was 1.8 wt%; this difference can be attributed to the amount of flame retardant Hexabromocyclododecane (HBCD) present in the original EPS. The presence of this type of flame retardant was confirmed by the FTIR analyses; see "Fourier-Transform Infrared Spectrometry (FTIR) Results" section. As expected, RW increased in the PPS and GPS samples, due to the presence of inorganic elements from glycerol and gypsum. The residual weight can be related to the amount of volatiles present in the samples, as volatiles are eliminated by heating the samples above the degradation temperature. Thus, the GPS sample contains a significantly lower amount of volatiles, since its residual weight (9%) was greater than that of the other compositions. These volatiles present in the samples can cause bubbles during processing, as can be seen in fabricated 3D printing filaments. The GPS filaments presented a more homogeneous and smoother surface, which facilitated the 3D printing of the specimens, while the other compositions presented bubbles along the surface of the filament produced, causing some difficulties in printing, such as breakage of filament, nozzle clogging, interruption in printing and reduction in processing speed [41].

Comparing the temperature of the RPS sample with the PS sample, as shown in Table 2, no significant change was observed, allowing to conclude that the recycling process did not change the thermal stability of the material. As reported by Maharana et al., this behavior indicates that the recycling process did not degrade the polymer and did not reduce its molar mass. Furthermore, the addition of glycerol increased the T_{onset} at 13 °C when compared with RPS and PPS samples. This event can be related to the volatility of the samples; since the PPS sample has less volatiles in its composition, it presents greater resistance to thermal degradation [18, 41].

Fourier-Transform Infrared Spectrometry (FTIR) Results

FTIR analyses were performed on all samples to identify the functional groups present and possible changes caused by processing and recycling. The spectra are presented in Fig. 3.

According to Fig. 3a, the appearance of some bands can be observed in the GPSin and GPS3d samples, which refer to the gypsum particles present in the composite. 1080 and 660 cm^{-1} refer to asymmetric stretching and asymmetric bending from sulphate ion, respectively, and 1620 cm^{-1} refers to H–O–H flexion from crystallization water molecules present in calcium sulphate hemihydrate [42]. Around 3600 cm^{-1} there is overlapping of the bands referring to O–H elongation from gypsum and glycerol [42, 43]. At 1450 cm^{-1}, there is another band overlap regarding the C–C stretching from the benzene ring (PS) and CH_2 bending from flame retardant and glycerol [44–46].

Figure 3b shows the comparison of FTIR Spectra between virgin polystyrene (PSin) and recycled EPS (RPSin and RPS3d) samples. In the region between 1300 and 800 cm^{-1}, the appearance of bands 1238, 1112, 980 and 880 cm^{-1} can be observed in the RPSin and RPS3d samples, referring to the stretching of the CC bond present in HBCD, thus proving that this was the retarder used during the manufacture of EPS samples, also confirmed in the results of the TG analyses shown in "Thermogravimetric (TG) Analyses Results" section. Other peaks referring to HBDC were found in the FTIR spectrum (Fig. 3a); between 600 and 700 cm^{-1} there are bands referring to C–Br stretching, and 841, 906, 942, 964, 980, 1001, 1027, 1046, 1068, 1112, 1152, 1180, 1197, 1238, 1310, 1328 cm^{-1} refer to C–C bending [44, 46].

The FTIR spectra show the samples do not have significant amounts of impurities as no unexpected band was detected. Another important finding is that there was no material degradation due to recycling, processing or printing, a fact confirmed by the absence of the band at 3440 cm^{-1}, regarding the oxidation of the benzene ring, which could be visible in samples without glycerol (PSin, RPSin and RPS3d), because this band could overlap the band by 3600 cm^{-1} corresponding to the stretch of OH bond present in glycerol, as can be seen in the Fig. 3a [43, 47]. The results show that all absorbed bands are in accordance with the data found in the literature and refer to PS, glycerol, gypsum, and flame retardant present in EPS.

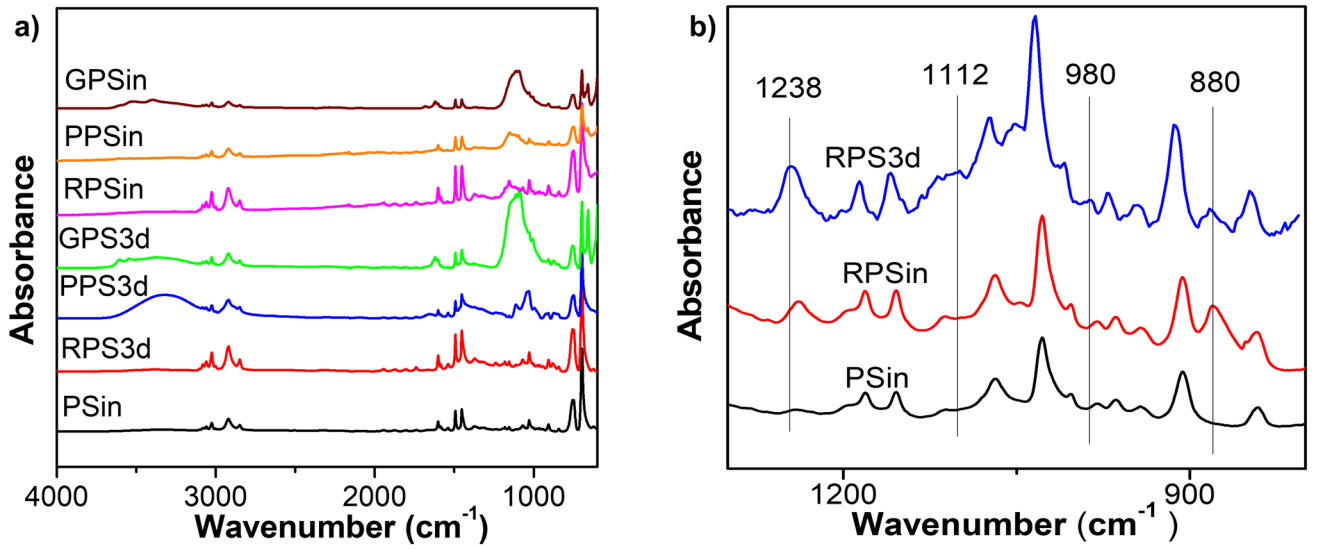

Fig. 3 **a** FTIR spectra of injected (PSin, RPSin, PPSin and GPSin) and 3D printed samples (RPS3d, PPS3d and GPS3d), between 4000 and 600 cm^{-1}; **b** FTIR spectra highlighting the appearance of HBCD bands between 1300 and 800 cm^{-1}, in the injected and 3D printed samples of Expanded Polystyrene Recycled (RPSin and RPS3d)

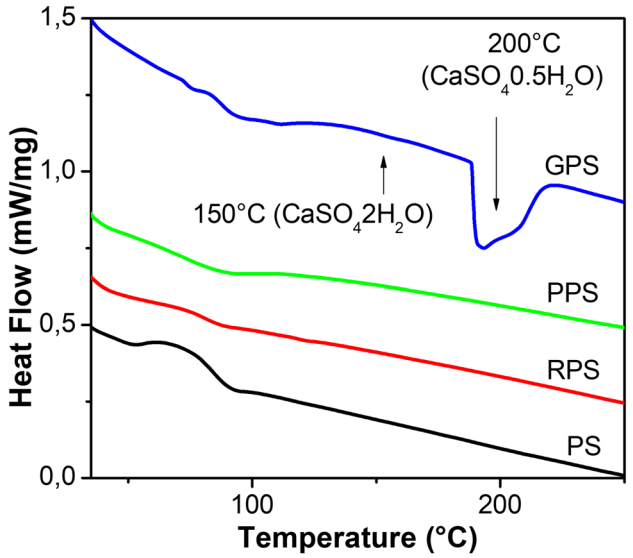

Fig. 4 DSC thermograms of Polystyrene (PS), Expanded polystyrene recycled (RPS), Expanded polystyrene recycled with 2 wt% glycerol as plasticizer (PPS) and Expanded polystyrene recycled with glycerol and 10 wt% gypsum (GPS). Highlighting the endothermic peaks of the GPS sample at 150 and 200 °C referring to $CaSO_4 2H_2O$ and $CaSO_4 0.5H_2O$, respectively

DSC

By observing the curves of the second heating cycle of the DSC assay, shown in Fig. 4, it was possible to identify the glass transition temperatures (Tg) of the samples, as shown in Table 3.

Table 3 Glass transition temperatures (Tg) of the samples

Sample	Tg (°C)
PS	84
RPS	88
PPS	80
GPS	88

The addition of glycerol reduced the polymer Tg from 88 to 80 °C, according to the results of samples RPS and PPS, respectively. This behavior was characteristic of a material with intrastructural plasticizer, which reduces the Tg of the polymer and increases its ductility, a result confirmed in the mechanical tests presented in "Tensile Tests Results" section. The reduction in Tg due to the addition of a plasticizer into amorphous polymers can be explained by the "Free Volume Theory". Free volume is the intern space not occupied by polymer chains, which increases with increasing temperature and provides mobility to the polymer. By heating the polymer from absolute zero (0 Kelvin), there is a sudden increase in free volume when Tg is reached, increasing flexibility and toughness. In fragile polymers such as PS, the Tg is above room temperature. Hence, when adding a plasticizer to the polymer, it is desirable that the Tg be reduced to obtain a more flexible polymer at room temperature. According to this theory, plasticizers increase the free volume of the material, maintaining it as the polymer is cooled from the melt, or from processing temperatures. That is, the plasticizer molecules fill the free volume of the polymer and prevent the formation of a rigid network during its cooling, increasing its toughness [27, 48].

However, for the mechanisms described above to act on the polymer, plasticizing it, the plasticizer must be compatible with the polymer. According to empirical tests carried out by Moorshead, the cohesion energy that binds the polymer molecules must be in the same order of magnitude as the plasticizer's cohesion. When the cohesive strength of the polymer is greater, the plasticizer cannot penetrate between the molecules and presents a droplet morphology in the polymeric matrix, not significantly reaching the expected plasticizer effect [49]. Furthermore, the polarity of the plasticizer and polymer must also be compatible, so that similar groups can interact, and toughening occurs by adding plasticizer. If the plasticizer is not compatible with the polymer, or if the mixture is not carried out correctly, plasticizer exudation may occur [48]. The plasticizer adherence to the polymer was achieved in the processing proposed herein and these results were confirmed by the mechanical tests and by the FESEM images presented in "Tensile Tests Results" and "Shore D Hardness" sections.

In the DSC analysis, the addition of gypsum to the composite resulted in the occurrence of an endothermic peak, around 200 °C, as highlighted in Fig. 4. This peak refers to the loss of the water molecule of calcium sulphate hemihydrate ($CaSO_4 0.5H_2O$), the main component of recycled gypsum. The absence of an endothermic peak around 150 °C, referring to calcium sulphate dihydrate ($CaSO_4 2H_2O$), shows that the proposed recycling process succeeded in completely transforming the post-consumer hydrated gypsum into a dehydrated structure ($CaSO_4 0.5H_2O$). During applications to civil construction, the hemi-hydrated gypsum ($CaSO_4 0.5H_2O$) is hydrated with water to present sufficient flexibility and grip so that it can be molded, transforming it into a dihydrated structure ($CaSO_4 2H_2O$). Hardening takes place between 15 and 20 min with a linear expansion of 0.3%. The reversible process of hydration and dehydration of gypsum enables its post-consumer recycling and is presented in Eq. 1 [50].

$$4CaSO_4 2H_2O + 23,81\frac{\text{cal}}{\text{g}} \leftrightarrow CaSO_4 0.5H_2O + 1.5H_2O \quad (1)$$

Comparing the PPS sample with the GPS sample, a 10% increase in Tg can be observed. This indicates that the interactions between the gypsum particles and the polymer can cause a partial immobilization of the polymeric chains and physical blockages in the molecular configurations in the vicinity of the particles, reducing molecular mobility and increasing Tg. This result corroborates the reduction of ductility presented in the mechanical tests presented in Chapter 3.4, whereby samples PPS3d and GPS3d are compared [51–54].

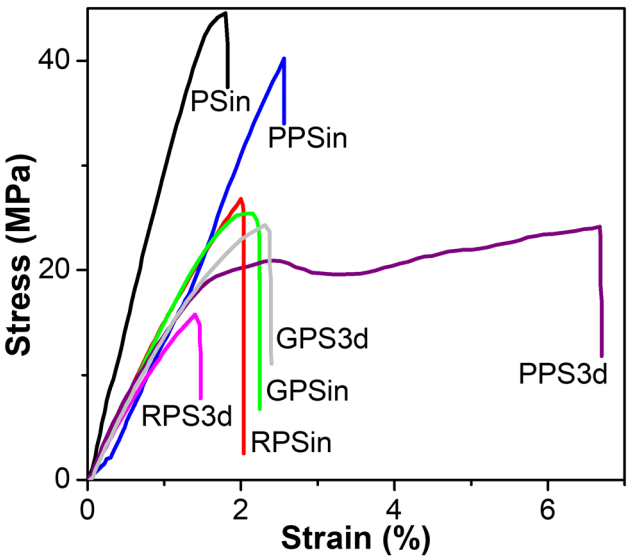

Fig. 5 Stress/strain curves from the tensile test of PSin, RPSin, PPSin, GPSin, RPS3d, PPS3d and GPS3d

Table 4 Mechanical properties (Tensile Strength at Break, elongation at break and Young's modulus) of virgin PS and recycled composition samples

Sample	Tensile Strength at Break (MPa)	Elongation at Break (%)	Young's modulus (MPa)
PSin	44.5 ± 0.8	1.8 ± 0.1	2974 ± 22
RPSin	26.8 ± 1.1	2.1 ± 0.1	1522 ± 17
PPSin	40.2 ± 2.6	3.2 ± 0.2	1371 ± 16
GPSin	26.2 ± 0.7	2.8 ± 0.2	1507 ± 14
RPS3d	15 ± 3.5	1.4 ± 0.3	1217 ± 20
PPS3d	24 ± 1.2	6.7 ± 0.3	1331 ± 19
GPS3d	24 ± 2.0	± 0.3	1507 ± 13

Tensile Tests Results

The stress/strain curves, obtained by averaging the tensile test results of 5 specimens of each composition (PSin, RPSin, PPSin, GPSin, RPS3d, PPS3d and GPS3d), are shown in Fig. 5 and, the resulting mechanical properties are shown in Table 4.

According to the results presented in Table 4, some comparisons can be made and are illustrated in the graph in Fig. S3. The PPSin sample had a tensile strength at break very close to the virgin PS sample, but with a 78% higher elongation at break. This shows that it is possible to obtain a recycled PS with a tensile strength close to the virgin material, but with a significant advantage, the increase of the material toughness, which minimizes the typical PS fragility problems.

Comparing the RPSin sample with the PPSin sample, there was a 50% increase in tensile strength at break, along with a 61% increase in elongation at break. These results prove the efficiency in toughening the RPS, by adding only 2 wt% of glycerol, and are in agreement with studies by other authors [27, 28].

Among the recycled samples, the highest Young's modulus found was the RPSin sample with a value of 1522 MPa. However, due to the fragility of the material, the values of strength and deformation at break were lower than the values of the PPSin sample.

In the GPSin sample, the addition of gypsum particles reduced the stress at break, leading to values close to the RPSin without glycerol. This occurs because the gypsum particles are weakly adhered to the polymer matrix, as shown in the FESEM images in "Shore D Hardness" section, and act as stress concentrators under mechanical strain, causing the material to break early, showing a fragile behavior [27, 55, 56].

Thus, the best mechanical behavior was found for samples toughened with glycerol plasticizer. The increase in stress at break due to the addition of glycerol can be justified, as the plasticizer reduced the glass transition temperature, increasing the mobility of polymer chains, which can induce a small and slow crystallization that results in the increased strength and toughened materials [57].

The significant increase in toughness, even with a low amount of plasticizer (2 wt% of glycerol) occurs because the plasticizer, with low molar mass chains, has a relatively high diffusivity and, therefore, can act at the interface between the polymeric matrix and microfibrils formed during plastic deformation of the polymer, reducing the tension in this region, and increasing the polymer toughness. Even though glycerol initially exhibits bubble morphology, as seen in FESEM images in "Shore D Hardness" section, during nucleation of microfibrils it can diffuse along the interface between the polymeric matrix and microfibrils, preventing growth and propagation of cracks [58].

Comparing the RPSin and RPS3d samples, there was a reduction in stress at break by approximately 40%, as well as a 10% reduction in the modulus of elasticity. These effects can be associated with the inherent voids of 3D printing manufacturing, as shown in the FESEM images in "Shore D Hardness" section.

However, there was an increase of 200% in the elongation at break of the PPS3d sample when compared to the same injected composition (PPSin), reaching 6.7% of deformation at the moment of rupture. The modulus of elasticity between these samples did not vary significantly, but the tensile strength at break was reduced by 50%. These results again showed that the empty spaces, in the morphology of the 3D printed specimen significantly affected the final properties of parts manufactured by this technology.

Evaluating the properties of the GPSin and GPS3d samples, no significant variations were found in the mechanical properties. This behavior can be attributed to the presence of gypsum particles, which prevented the formation of bubbles during the manufacture of the filament and during 3D printing, made the filament more uniform and printing faster, easier and without interruptions, as happened with the other samples of this work. Thus, filaments with less variation in diameter and better surface roughness confirmedly allowed for more stable 3D printing, reflecting in better final properties of the parts manufactured by this additive technology, which can be similar to the properties of injected materials [8, 59, 60]. It is therefore possible to value the REPS through the manufacture of filaments for printing, enabling economically viable recycling.

The recycled EPS sample with gypsum enabled to print specimens with mechanical properties similar to the injected sample; it would hence be feasible to apply this composition to manufacture recycled filaments for prototype printing in various areas, such as mechanical engineering, medicine and orthodontics. PLA is currently used for this type of application due to its ease of 3D printing, but this material has a high cost. By replacing PLA with GPS3d, there will likely be a reduction in material cost, as post-consumer EPS is a low-cost material.

Price Estimate

The cost of the filament produced for 3D printing proposed herein can be estimated for comparison with commercial PLA (polylactic acid) filaments. According to what was presented in Table 5, to estimate the price of 1 kg of filament manufactured with the GPS sample, it was considered:

- Prices in Brazil in February 2022, found on the internet search page.
- Reuse of the ethyl acetate solvent with 90% utilization.
- Minimum wage in Brazil of R$1212.00 with a 44-h workweek.
- Residential energy value of R$0.71/kWh
- Mechanical mixer used for 2 h with 40 W of power
- Extruder used for 30 min with 7kWh of power
- 30% profit.

According to Table 5, the price for manufacturing 1 kg of filament with the GPS sample was R$77.27, while commercial PLA filaments are sold at R$115. The results show

Table 5 Price estimate for manufacturing 1 kg of filament for 3D printing produced with the GPS sample

Component	Provider	Quantity	Price (R$)	Quantity x Price
Ethyl acetate	ACS Reagentes	2 L (90% reusable)	176.58 × 0.1	R$35.23
Glycerol	Casa do Químico	0.02 L	21.34	R$0.43
Gypsum	Leroy Merlin	0.1 kg	1.00	R$0.10
EPS	Knauf	1 kg	0.50	R$0.50
Energy expenditure with the mechanical mixer	CPFL	40 W × 2 h	0.71/kWh	R$0.03
Energy expenditure with the extruder	CPFL	7 kW × 30 min	0.71/kWh	R$2.49
Labor	Governo Federal do Brasil	3 h	1212.00/month	R$20.66
Profit				30%
			TOTAL	R$77.27

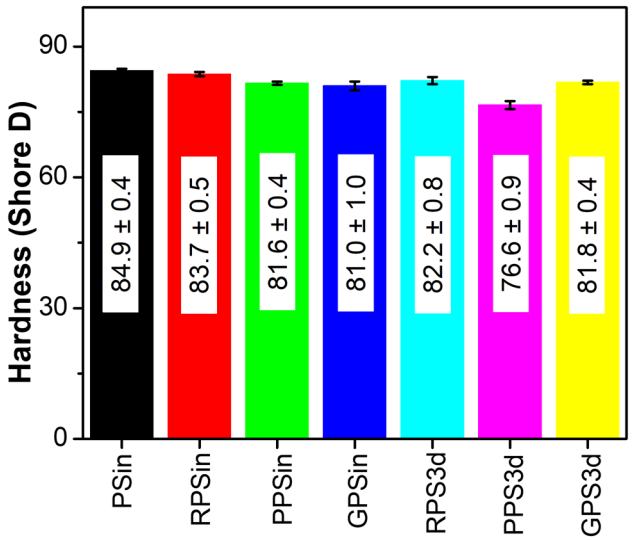

Fig. 6 Shore D hardness results (means and standard deviations) of all samples

a reduction in price of approximately 33%. That is, the proposed process, even on a small scale, will produce an environmentally friendly and cheaper product for the final consumer.

Shore D Hardness

In each composition, 10 hardness measurements were performed on the Shore D scale, the means and standard deviations are shown in Fig. 6.

According to the data presented, comparing the samples with (PPSin and PPS3d) and without plasticizer (RPSin and RPS3d), the addition of glycerol reduced the hardness of the material, but there were significant gains in the tensile strength of these samples as discussed in "Tensile Tests Results" section. Consequently, the reduction in hardness of this material should not be interpreted as a loss of property: as PS is a very brittle material, a reduction in hardness can result in a more ductile and flexible material, as proven by tensile tests. The addition of recycled gypsum particles also reduced the hardness of PSGin but increased the hardness of PSG3d. Comparing the injected and printed samples, there was a variation of up to 6%.

Results of the Field Emission Scanning Electron Microscopy (FESEM) Analyses

The FESEM micrographs allowed visualizing the morphology of the materials and the dispersion of particles in the polymeric matrix; the images obtained are shown in Figs. 7, 8, and 9.

Figure 7 shows micrographs of the RPSin sample (a and b), with glycerol without extruder processing (c and d) and with glycerol (PPSin) processed in an extruder (e and f). The polymeric matrices of Fig. 7a, b, e, and f showed a roughness in the form of small whitish spheres, which appeared in the material due to the formation of bubbles, caused by the volatilization of the blowing agent, during heating and processing in an extruder [61, 62]. In Fig. 7c and d, the processing in an extruder was not used, which made the sample surface smoother, but the porosity present in the sample is greater when compared to the PPSin sample, which was processed in an extruder. The pore size was measured using the Image J software, and the mean found was 3 ± 0.5 and 1 ± 0.2 µm, respectively, that is, the extrusion reduced the

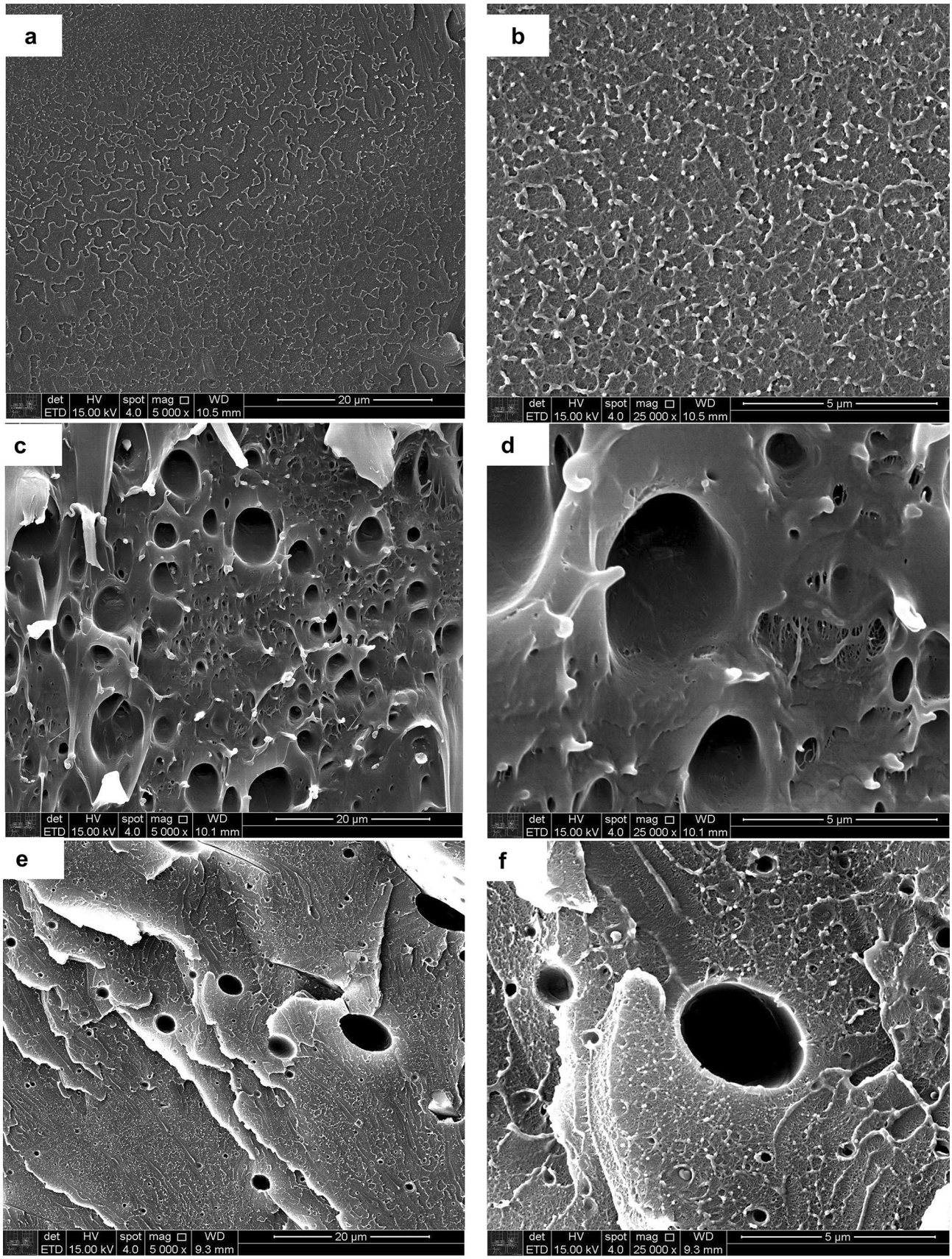

Fig. 7 FESEM micrographs of samples RPSin (**a**, **b**), PPSin without extrusion (**c**, **d**) and PPSin (**e**, **f**), with 5000 and 25,000 times magnification, respectively

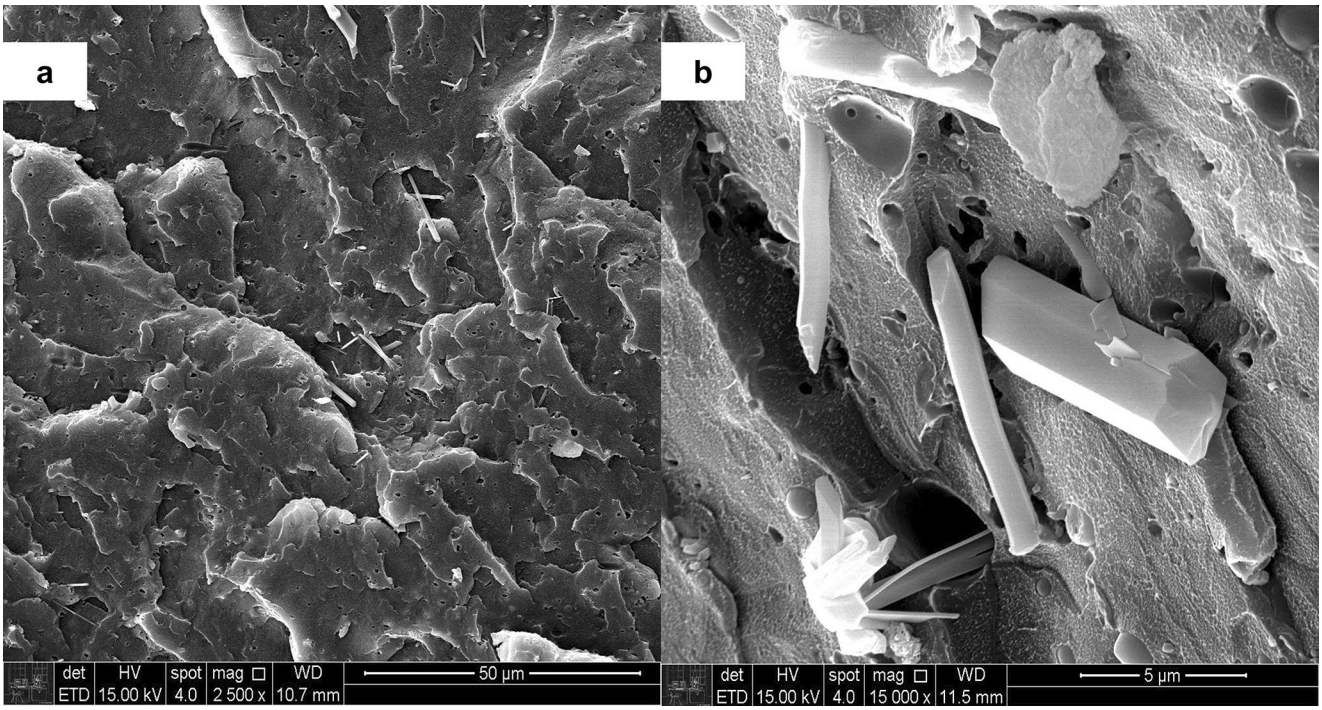

Fig. 8 FESEM micrographs of samples GPSin (**a**, **b**) with 2500× and 15,000× magnification, respectively

pore size and leveled the glycerol distribution in the polymeric matrix.

In Fig. 8, the micrographs obtained by FESEM of the GPSin sample (a and b) with magnification of 2500 and 15,000 times are shown. Observing the micrographs, it could be noted that the gypsum particles presented rectangular stick shapes, which are isolated and uniformly distributed in the polymeric matrix. However, the particles show not to be embedded by the polymer, causing empty spaces between the particles and the matrix. Furthermore, many particles broke off during the cryogenic rupture, leaving voids on the analyzed surface of the composite. Thus, it can be stated that the adhesion of gypsum particles to RPS is weak, corroborating the loss of properties verified in mechanical tests. In the images, it was also possible to observe the morphology of the polymeric matrix, which remained constant, with some rounded voids evenly distributed.

In Fig. 9, the FESEM micrographs obtained from the samples printed in 3D, RPS3d (a, b), PPS3d (d) and GPS3d (f) and of the injected samples RPSin (c), PPSin (e) and GPSin (g) at 500× magnification, except for micrograph 10a, which was taken at 100× magnification. Looking at micrograph 10a, empty spaces can be seen, highlighted by rectangles. These empty spaces are unavoidable due to the manufacturing method, even if the filling is 100%. This filling percentage defines the distance at which the print lines will be deposited on the table; if one line is tangent to another, the percentage is 100%. However, due to the round shape of the filament, even tangent to lines and overlapping layers, form voids in the structure of the specimen or parts printed in 3D.

FESEM micrographs 10b and 10c showed the polymeric matrix without the presence of pores of samples RPS3d and RPSin, respectively. The empty space, highlighted by the rectangle in 10b, is the spacing between the 3D print lines.

The glycerol-containing samples showed pores in the polymer matrix for injected and 3D-printed samples, as highlighted by the circles in the 10d, 10e, 10f, 10g images. However, the 3D printed sample containing plaster (GPS3d, 10f image) had excessively larger pores than the injected sample (GPSin, 10g image), as highlighted by the circles. However, even with this greater number of pores in the fracture region, the mechanical properties of the samples were similar. It can hence be concluded that this porosity is not representative of the GPS3d sample. The filament with better dimensional and roughness control was obtained with the sample containing gypsum particles (GPS3d). These characteristics enabled a faster and uninterrupted printing, which led the printed material to have similar properties to those of the injected material, even with the presence of voids intrinsic to additive manufacturing.

Flame Propagation Test

The injected samples underwent the flame propagation test by horizontal burning. The specimens flame propagation time and burnt length were measured to calculate the burn rate (V) in mm/min. To perform the test, the specimen was subjected to a flame for 30 s, then the flame was stopped and the behavior of the material was observed. In Table 6, the burnt length was recorded after the incidence of the flame for 30 s, adding the burnt length until the flame self-extinguished or until the flame reached 100 mm. The time shown in the table refers to the time it took for the flame to reach 100 mm or to be extinguished by the material, subtracting the initial 30 s whereby the flame was acting on the material, in accordance with the ASTM D635 standard. Table 6 shows the results, as well as the mean and standard deviation of the burning rate. In the sample column, the data marked with (*) means that the burn did not reach 100 mm, as the specimen was consumed by the flame, becoming very small and falling off the support.

Studies show that the addition of gypsum to polymeric composites can reduce the burning rate because the gypsum acts through the barrier mechanism, as occurs with the addition of clay and other ceramics. This mechanism suggests that particles migrate to the bubble surfaces of molten polymers due to the action of the flame. The particles degrade forming a multi-layered carbon silica structure on the surface of the nanocomposite that protects the substrate from heat and oxygen, delays the escape of flammable volatiles generated during polymer degradation, reducing the heat release rate of the nanocomposite compared to the pure polymer. This also reduces the rate of weight loss, reducing flame propagation and increases the thermal stability of the polymer matrix [63–69]**.** However, this did not occur with the samples analysed in the present work. As can be seen in Table 6, the burn rate of the GPSin sample was 2.5 times higher than the burn rate of the PSin sample. This is because the GPSin sample was obtained with recycled EPS and 10 wt% gypsum was added. The addition of gypsum reduced the percentage of flame retardant present in the original material (EPS). In addition, commercial EPS is manufactured with the addition of a blowing agent, typically a chlorinated hydrocarbon or a low-boiling petroleum-derived agent with the presence of pentane. These substances are highly flammable; by reducing the amount of flame retardant due to the addition of gypsum, they ignited during the flame propagation test, increasing the burn rate of the GPSin sample [61, 62, 70, 71].

The recycled samples without gypsum addition maintained the self-extinguishing flame, resulting from the action of the flame retardant (HBCD) present in the EPS residue used in this work. However, when adding gypsum particles to the RPS, the material did not resist the flame, propagating it, eliminating smoke and soot during combustion, which consumed the entire length (100 mm) of the specimen. According to the D635 standard, the material can be classified as HB (horizontal burning) if there is no visible sign of combustion after removing the ignition source, as occurred in the RPSin samples. This result can be seen in the video available in the Supplementary Information.

According to the results presented and discussed, this work proposes two application areas for recycled class II EPS, 3D printing and civil construction. Many applications to civil construction require the material to be flame retardant, which was possible to obtain in the recycled EPS sample with glycerol. This composition could be used for manufacturing profiles, roof wheels, foot wheels, finishing boards, ceiling lining, among others. Traditionally, these civil construction internal finishing items are manufactured with plasterboard. Plaster or gypsum, in turn, is a material that does not propagate flames in the event of fire, and can

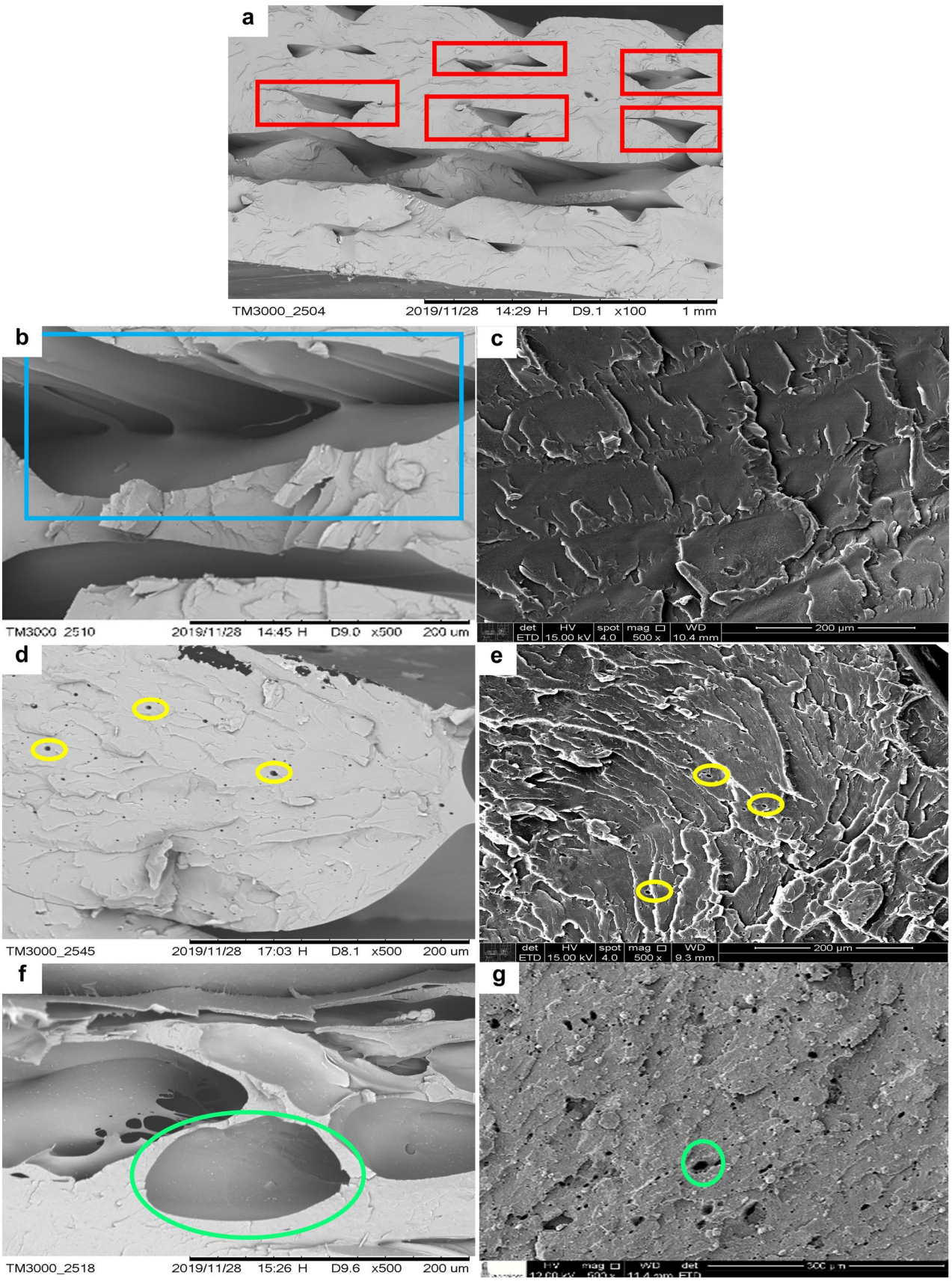
a
TM3000_2504 2019/11/28 14:29 H D9.1 x100 1 mm
b
TM3000 2510 2019/11/28 14:45 H D9.0 x500 200 um
c
det HV spot mag WD
ETD 15.00 kV 4.0 500 x 10.4 mm
200 µm
d
TM3000_2545 2019/11/28 17:03 H D8.1 x500 200 um
e
det HV spot mag WD
ETD 15.00 kV 4.0 500 x 9.3 mm
200 µm
f
TM3000_2518 2019/11/28 15:26 H D9.6 x500 200 um
g

◂**Fig. 9** FESEM micrographs of samples printed in 3D [RPS3d (**a**, **b**), PPS3d (**d**) and GPS3d (**f**)] and injected [RPSin (**c**), PPSin (**e**) and GPSin (**g**)], with 500× magnification, except for micrograph 10a, which was taken at 100× magnification

be classified as self-extinguishing as well as sample PPS [72–74].

Conclusions

The present study focuses on recycling expanded polystyrene using a biodegradable solvent, its plastification with glycerol, and the preparation of the composite with post-consumer recycled gypsum for manufacturing 3D printed prototypes. The post-consumer gypsum could be calcined at 100 °C due to the particle size facilitating the removal of the structural water present in the sample before calcination. EPS recycling can be performed, without degradation, using biodegradable ethyl acetate to reduce the sample volume, for further processing in an extruder. The reduction in the volume of material results in a reduction in transport and storage costs for the recycling industries. The plastification of recycled EPS improved its mechanical properties and thermal stability, besides maintaining flame self-extinguishment during flame propagation tests. While the addition of gypsum increased the thermal stability, it facilitated the propagation of flames in the material. The 3D printing of the recycled materials was possible, but the greater dimensional stability of the GPS filament improved the print quality, resulting in final properties of the 3D printed parts similar to the injected parts. Then, according to these results, the plasticized composite material prepared is suitable for both manufacturing articles for finishing in civil construction, and also for manufacturing 3D printed prototypes.

Table 6 Results of the flame propagation test

Sample	Nº	Burnt length (mm)	Time (s)	Burn rate (mm/min)	Mean (mm/min)	Standard deviation
PSin	1*	90	240	22.5	23.4	1.3
	2*	85	210	24.3		
RPSin	1	35	0	Flame self-extinguished		
	2	40	0			
	3	35	0			
PPSin	1	30	12	Flame self-extinguished		
	2	30	1			
	3	30	12			
GPSin	1*	75	76	59.2	58.4	1.1
	2*	75	78	57.7		

*During flame propagation the sample became too small, fell off the support and stopped the test

Supplementary Information The online version contains supplementary material available at https://doi.org/10.1007/s10924-022-02465-7.

Acknowledgements To professors Maria Cristina Vidal Borba from USP and Ricardo José Orsi de Sanctis from Fatec Sorocaba for the reviews.

Funding This work was supported by FAPESP (Process Number 2019/00862-9), CAPES, and CNPq.

Declarations

Conflict of interest The authors have not disclosed any competing interest.

References

1. Qin ZH et al (2021) Biotechnology of plastic waste degradation, recycling, and valorization: current advances and future perspectives. Chemsuschem 14:13
2. ABIPLAST. PERFIL 2020. Available at http://www.abiplast.org.br/wp-content/uploads/2021/08/Perfil2020_abiplast.pdf
3. Idumah CI, Nwuzor IC (2019) Novel trends in plastic waste management. SN Appl Sci 1(11):1–14
4. Browning S, Beymer-Farris B, Seay JR (2021) Addressing the challenges associated with plastic waste disposal and management in developing countries. Curr Opin Chem Eng 32(100682):7
5. Park S, Fu KK (2021) Polymer-based filament feedstock for additive manufacturing. Compos Sci Technol 213(108876):14
6. Tan LJ, Zhu W, Zhou K (2020) Recent progress on polymer materials for additive manufacturing. Adv Func Mater 30(43):1–54
7. Zander NE et al (2019) Recycled polypropylene blends as novel 3D printing materials. Addit Manuf 25:122–130
8. Spoerk M et al (2019) Mechanical recyclability of polypropylene composites produced by material extrusion-based additive manufacturing. Polymers 11(8):1318
9. ABIQUIM. **EPS BRASIL**. Available at http://www.epsbrasil.eco.br/noticia/view/38/reciclagem-e-transformacao-do-eps-pos-consumo-em-novos-produtos-e-solucoes.html. Accessed on 22 May 2018
10. Pieronia MC, Leonelb J, Fillmanna G (2017) Retardantes de chama bromados: uma revisão. Quim Nova 40(3):317–326
11. Gallo JB, Agnelli JAM (1998) Aspectos do comportamento de polímeros em condições de incêndio. Polímeros 8:23–38
12. Ministry of Environment (2015) National implementation plan Stockolm convention. In: Brazilian Institute of Environment and Natural Renewable Resources
13. Irvine DJ, McCluskey JA, Robinson IM (2000) Fire hazards and some common polymers. Polym Degrad Stab 67(3):383–396
14. ABNT—Associação Brasileira De Normas Técnicas (2007) NBR11948—Poliestireno expandido para isolação térmica—Determinação de flamabilidade. Rio de Janeiro
15. European Manufacturers of EPS. Behaviour of EPS in case of fire. Available at http://osfm.fire.ca.gov/codedevelopment/pdf/wgfsbim/EUMEPS_FireBehavior.pdf. Accessed on 11 Apr 2016
16. Secretaria Do Estado Dos Negócios Da Segurança Pública. Polícia Militar (2011) Instrução Técnica n° 10—Controle de materiais de acabamento e de revestimento. Corpo de Bombeiros. pp 217–226
17. Secretaria Do Estado Dos Negócios Da Segurança Pública. Polícia Militar (2011) Instrução Técnica n° 08—Resistência ao fogo dos elementos de construção. Corpo de Bombeiros. pp 191–202
18. Maharana T, Negi YS, Mohanty B (2007) Review article: recycling of polystyrene. Polym-Plast Technol Eng 46(7):729–736
19. ERCROS. Acetato de Etilo. Available at http://www.ercros.es/index.php?option=com_docman&task=doc_download&gid=753&Itemid=647. Accessed on 1 Jan 2016
20. Singhal R, Ishita I, Sow PK (2019) Integrated polymer dissolution and solution blow spinning coupled with solvent recovery for expanded polystyrene recycling. J Polym Environ 27(6):1240–1251
21. Cella RF et al (2018) Polystyrene recycling processes by dissolution in ethyl acetate. J Appl Polym Sci 135(18):1–7
22. Yoshida E, Terada Y (2005) Micelle formation of a nonamphiphilic poly(vinylphenol)-block-polystyrene diblock copolymer in ethyl acetate. Colloid Polym Sci 283(11):1190–1196
23. Sarkis CE (2009) Reciclagem de poliestireno expandido (EPS) para uso na fabricação de perfilados de poliestireno (PS). Universidade Federal de Santa Catarina, Florianópolis
24. Borsoi C (2012) Compósitos de poliestireno e poliestireno expandido reciclado reforçado com fibras de curauá: propriedades e degradação. Universidade de Caxias do Sul, Caxias do Sul
25. Caraschi JC, Leão AL (2002) Avaliação das propriedades mecânicas dos plásticos reciclados provenientes de resíduos sólidos urbanos. Acta Sci 24(6):1599–1602
26. Brydson JA (1995) Plastics based on styrene. Plastics materials, 6th edn. British Plastics and Rubber, Oxford, pp 410–448
27. Sjoerdsma SD (1986) The effect of glycerol on the crazing behaviour of polystyrene in relation to the craze boundary temperature. Polymer 27(2):164–168
28. Andreson T (2005) Elastic-plastic fracture mechanics. Fracture mechanics: fundamentals and applications, 3rd edn. Taylor & Francis, Boca Raton, pp 117–182
29. Schlemmer D, Sales MJA, Resck IS (2010) Preparação, caracterização e degradação de blendas PS/TPS usando glicerol e óleo de buriti como plastificantes. Polímeros 20(1):6–13
30. Schlemmer D, de Oliveira ER, Sales MJA (2007) Polystyrene/thermoplastic starch blends with different plasticizers: preparation and thermal characterization. J Therm Anal Calorim 87(3):635–638
31. Peng Z, Ma L, Gong X (2014) Comparison of life cycle environmental impacts between natural gypsum board and FGD gypsum board. Key Eng Mater 599:15–18
32. U.S. Geological Survey (2017) Mineral commodity summaries 2017, 1st edn. U.S. Geological Survey, Washington
33. Lima TM, Neves CAR (2016) Sumário mineral 2015. Departamento Nacional de Produção Mineral, Rio de Janeiro
34. Machado MDS (2016) Nanocompósito de poliestireno reciclado, bentonita sódica e hemi-hidrato de sulfato de cálcio: obtenção e Caracterização. Universidade de São Paulo, São Paulo
35. Madariaga FJG, Macia JL (2008) Mezclas de residuos de poliestireno expandido (EPS) conglomerados con yeso o escayola para su uso en la construcción. Inf Constr 60(509):35–43
36. Erbs A et al (2018) Properties of recycled gypsum from gypsum plasterboards and commercial gypsum throughout recycling cycles. J Clean Prod 183:1314–1322
37. Jiménez-Rivero A, García-Navarro J (2017) Characterization of quality recycled gypsum and plasterboard with maximized recycled content. Mater Constr 67(328):137
38. Bartolomei SS, Wiebeck H (2019) Characterization of gypsum waste from civil construction to obtain polymer composites. Mater Sci Forum 958 MSF(1):47–51
39. Kruis AJ et al (2017) Ethyl acetate production by the elusive alcohol acetyltransferase from yeast. Metab Eng 41:92–101
40. Gutiérrez TJ, Alvarez VA (2017) Properties of native and oxidized corn starch/polystyrene blends under conditions of

reactive extrusion using zinc octanoate as a catalyst. React Funct Polym 112:33–44
41. Murariu M et al (2008) Polylactide (PLA)-$CaSO_4$ composites toughened with low molecular weight and polymeric ester-like plasticizers and related performances. Eur Polym J 44(11):3842–3852
42. Wei Y et al (2016) The ftir fingerprint of *Gypsum fibrosum*. Acta Med Mediterr 32:607–611
43. Zuhaimi NAS et al (2015) Reusable gypsum based catalyst for synthesis of glycerol carbonate from glycerol and urea. Appl Catal A 502:312–319
44. Zhang K et al (2014) Mechanochemical degradation of hexabromocyclododecane and approaches for the remediation of its contaminated soil. Chemosphere 116:40–45
45. Jiang L et al (2019) Direct introduction of elemental sulfur into polystyrene: a new method of preparing polymeric materials with both high refractive index and Abbe number. Polymer 180:121715
46. Lin-Vien D et al (1991) The handbook of infrared and Raman characteristic frequencies of organic molecules. Academic Press, Londres
47. Ani KEAL, Ramadhan AE (2015) Kinetic study of the effect of plasticization on photodegradation of polystyrene solid films. Mater Sci Appl 6:617–633
48. Bocqué M et al (2016) Petro-based and bio-based plasticizers: chemical structures to plasticizing properties. J Polym Sci Part A Polym Chem 54(1):11–33
49. Moorshead TC (1962) Advances in PVC compounding and processing, 1st edn. M. Kaufman and Sons, London
50. Preturlan JGD et al (2020) Kinetics and mechanism of the dehydration of calcium sulfate dihydrate: a comprehensive approach for studying the dehydration of ionic hydrates under controlled temperature and water vapor pressure. J Phys Chem C 124(48):26352–26367
51. Yim A, Chahal RS, Pierre LES (1973) The effect of polymer-filler interaction energy on the T′g of filled polymers. J Colloid Interface Sci 43(3):583–590
52. Alekseeva OV, Noskov AV, Guseynov SS (2020) Thermal behavior of polystyrene-based composite materials. Prot Met Phys Chem Surf 56(3):469–472
53. Ajji Z (2005) Preparation of polyester/gypsum/composite using gamma radiation, and its radiation stability. Radiat Phys Chem 73(3):183–187
54. Firmino HCT et al (2017) Caracterização de compósitos particulados de polietileno de alta densidade/pó de concha de molusco. Rev Mater. https://doi.org/10.1590/s1517-707620170004.0213
55. Argon AS, Cohen RE, Mower TM (1994) Mechanisms of toughening brittle polymers. Mater Sci Eng A 176(1–2):79–90
56. Kinloch AJ, Yung RJ (1995) Glassy polymers I—thermoplastics. Fracture behaviour of polymers, 5th edn. Champman and Hall, London, pp 229–285
57. Velasquez D et al (2015) Effect of crystallinity and plasticizer on mechanical properties and tissue integration of starch-based materials from two botanical origins. Carbohydr Polym 124:180–187
58. Plummer CJG, Donald AM (1990) Disentanglement and crazing in glassy polymers. Macromolecules 23(17):3929–3937
59. Lee C-Y, Liu C-Y (2019) The influence of forced-air cooling on a 3D printed PLA part manufactured by fused filament fabrication. Addit Manuf 25:196–203
60. Bakrani Balani S et al (2019) Influence of printing parameters on the stability of deposited beads in fused filament fabrication of poly(lactic) acid. Addit Manuf 25:112–121
61. Soykeabkaew N, Thanomsilp C, Suwantong O (2015) A review: starch-based composite foams. Compos A Appl Sci Manuf 78:246–263
62. Eaves D (2004) Handbook of polymer foams 1, Ed. Rapra, Shawbury
63. Kareem Salih W (2019) Flame retardancy properties and thermomechanical behavior of the nanocomposite of thermoplastic polypropylene/linear low-density polyethylene blend filled with nano calcium carbonate. J Phys Conf Ser 1294(5):052020
64. Kiliaris P, Papaspyrides CD (2010) Polymer/layered silicate (clay) nanocomposites: an overview of flame retardancy. Prog Polym Sci (Oxford) 35(7):902–958
65. Laoutid F et al (2009) New prospects in flame retardant polymer materials: from fundamentals to nanocomposites. Mater Sci Eng 63(3):100–125
66. Leszczyńska A et al (2006) Polymer/montmorillonite nanocomposites with improved thermal properties. Thermochim Acta 453(2):75–96
67. Morgan AB (2006) Flame retarded polymer layered silicate nanocomposites: a review of commercial and open literature systems. Polym Adv Technol 17(4):206–217
68. Morgan AB et al (2003) Flammability of polystyrene layered silicate (clay) nanocomposites: carbonaceous char formation. Fire Mater 26(6):247–253
69. Ning W, Jiugao Y, Xiaofei M (2008) Review new developments in flame retardancy of styrene thermoplastics and foams. Polym Int 57:431–448
70. Fayet G, Tribouilloy B, Rotureau P (2020) Flash point of binary mixtures of chlorinated hydrocarbons with toluene and their predictability with existing mixing rule. Process Saf Prog. https://doi.org/10.1002/prs.12127
71. Grimminger J, Muha K (1995) Silicone surfactants for pentane blown rigid foam. J Cell Plast 31(1):48–72
72. Rahmanian I, Wang YC (2012) A combined experimental and numerical method for extracting temperature-dependent thermal conductivity of gypsum boards. Constr Build Mater 26(1):707–722
73. Kolaitis DI, Founti MA (2013) Development of a solid reaction kinetics gypsum dehydration model appropriate for CFD simulation of gypsum plasterboard wall assemblies exposed to fire. Fire Saf J 58:151–159
74. Bryner NP, Mulholland GW (1991) Smoke emission and burning rates for urban structures. Atmos Environ A 25(11):2553–2562